Applied Sciences, Computing and Energy, 2025, 3(2), 212-223

High durability, stability, effective thermoelectric and thermodynamic properties of NbFePb half-Heusler compound

Ayedun, Funmilayo*, Adetunji Bamidele Ibrahim, Solola, Gbenro Timothy, Bamgbose, Matthew Kehinde, Adebambo, Paul Olufunsho, Agbaoye, Ridwan Olamide, Mansur Said, Nwachukwu, Iheke Michael

Received : 11 July 2025/Accepted : 22 August 2025/Published online : 05 September 2025

Abstract*: We examined structural, electronics, elastic, mechanical and thermodynamic properties of an innovative NbFePb compound using the ultrasoft pseudopotential and nonlinear core correction functional type of Perdew-Burke-Ernzenhof as specified in Quantum Espresso soft bundles in line with density functional theory with the atomic framework of Generalized Gradient Approximation. The transport behaviours were determined by engaging semi-classical Boltzmann transport theory as detailed in Boltz Trap code. The calculated lattice constant is 5.50Å. The computed electronic band structure has an indirect energy gap of 1.4 eV between points Γ and X revealing a semiconductor compound. Total and partial density of states were explored and this reflect the dominance of Pb p-atom. The high value of ratio of bulk modulus to shear modulus (5.01), Poisson ratio (0.44), and positiveCauchy's pressure (239.49GPa) indicate durability and capacity of this material to resist deformation under stress.NbFePb is an anisotropic compound with universal anisotropic greater than one. Debye temperature of 296.48K was recorded. NbFePb compound exhibited esteemed value of Seebeck coefficient 2516.96μV/K at 300K, premium power factor of 21.02 x10^{10}W/msK^2 at 800K and Fig. of merit 21.09 also at 800K. This makes this material to have a high-potential for thermoelectric purposes.*

Keywords*: NbFePb, Half –Heusler, Seebeck coefficient, Density Functional Theory, Thermodynamic properties*

Ayedun, Funmilayo*
Department of Physics, National Open University of Nigeria
Email: fayedun@noun.edu.ng
Orcid id: https://orcid.org/0000-0001-5421-9305

Adetunji, Bamidele Ibrahim
Department of Physics, The Bells University, Ota, Nigeria
Email: bamideleibrahim@yahoo.com
Orcid id: https://orcid.org/0000-0002-2097-6612

Solola, Gbenro Timothy
Department of Physics, Augustine University, Ilara-Epe, Nigeria
Email: gsolola2050@gmail.com
Orcid id: https://orcid.org/0000-0003-2629-5858

Bamgbose, Matthew Kehinde
Department of Physics, Lagos State University, Ojo, Nigeria
Email: muyiwa.bamgbose@lasu.edu.ng
Orcid id: https://orcid.org/0000-0002-6080-9579

Adebambo, Paul Olufunsho
Department of Physics, Federal University of Agriculture, Abeokuta, Nigeria
Orcid id : https://orcid.org/0000-0002-2066-0757

Agbaoye, Ridwan Olamide
Centro de Física de Materiales, Donostia San Sebastian, Spain
Email: ridwanolamide.agbaoye@ehu.eus
Orcid id: https://orcid.org/0000-0002-5629-6846

Said Mansur
Department of Physics, Bayero University, Kano
Email: mansursaid79@gmail.com
ORCID ID: https://orcid.org/0000-0002-8743-9248

Nwachukwu, Iheke Michael
Department of Physics, National Open University of Nigeria
Email: inwachukwu@noun.edu.ng
Orcid id: https://orcid.org/0000-0003-2237-7805

1.0 Introduction

Survey on half-Heusler (HH) compounds is on the rise because of their ability to produce an eco-friendly, green and renewable energy which is cost effective with present global surge in fossil fuel price. HH finds usage in spintronics (Casper *et al*, 2012), magnetic sensors, thermoelectric and energy conversion. The energy conversion from waste is enhanced due to high power factor, meaningful Fig. of merit and low thermal conductivity.

Transition metals conform to an eighteen-electron rule because the addition of metal d electrons and the electrons conventionally evaluated as being presented by the neighbouring ligands amount to 18. This rule is crucial in predicting structure and reactivity of molecules and organometallic complexes. Transition metal or rare metal complexes such as I-X-VII, II-IX-VII, II-IX-VIII and III-IX-VI (Grautier *et al*., 2015) are said to be saturated and cannot bind electronically to additional ligands. NbFePb comply with 18 valence electron rule and crystalize into face centred cubic lattice of MgAgAs structure type.

Machinability and stability of materials are needed tools for determining materials which require little power consumption, accurate finish quality and so on. Mechanical properties of materials comprise of elastic properties, hardness and strength, fracture toughness and ductility (Everhart and Newkirk, 2019, Murugan, 2020, Mokhtari *et al*., 2023) and have applications in the field of Engineering. These features are investigated in this study using density functional theory (Mogulkoc and Ciftci, 2017; Mohan *et al*., 2020; Ciftci, 2021; Missoum *et al*., 2022; Solola *et al*., 2023).

Some researchers (Khandy *et al*., 2021; Lv *et al*., 2024; Serrano-Sanchez *et al*., 2020) probed materials which are capable of converting waste heat into a form of renewable energy, considering factors such as enhanced Seebeck coefficient (S), improved Fig. of merit (zT), high power factor (PF) and low thermal conductivity (k) have investigated different HH compounds such as NbCoSn, PtZrSn, PtHfSn, RbMgSb, LiMgSb. Despite the remarkable progress in the investigation of half-Heusler compounds, the NbFePb system remains largely unexplored in both theoretical and experimental studies. Unveiling the fundamental properties of NbFePb is significant because it can broaden the family of half-Heusler compounds with potential applications in renewable energy conversion, thermoelectric devices, and spintronic technologies. Establishing its structural stability, electronic features, and transport behavior provides not only a foundation for future experimental validation but also guidance for the rational design of novel materials that contribute to sustainable and eco-friendly energy solutions

2.0 Method

First-principles computations were carried out using projector augmented wave (PAW) pseudopotentials within the framework of density functional theory (DFT), as implemented in the Quantum ESPRESSO package (Giannozzi *et al*., 2009; Giannozzi *et al*., 2017). The Perdew–Burke–Ernzerhof (PBE) exchange–correlation functional, based on the generalized gradient approximation (GGA), was adopted because it is cost- and time-efficient while providing reliable results.

A 3 × 3 × 3 k-point mesh was used for structural optimization and electronic band structure calculations. For self-consistent plane-wave calculations, the energy cutoff was set to 120 Ry. A denser 24 × 24 × 24 k-point grid was employed to evaluate the thermoelectric properties by solving the Boltzmann semi-classical transport equations using the BoltzTraP code (Madsen, 2006; Ayedun, 2024).

3.0 Results and Discussion

3.1 Structural and Electronic Properties

The NbFePb compound crystallizes into a face-centered cubic structure with equal lattice parameters (a = b = c). The optimized atomic positions place Nb, Fe, and Pb at (0.50, 0.50, 0.50), (0.25, 0.25, 0.25), and (0.00, 0.00, 0.00), respectively. The total energies as a function of lattice constant revealed an equilibrium lattice parameter of 5.50 Å. This value lies well within the reported range for half-Heusler alloys (5.29–6.43 Å), indicating structural consistency and stability (Zhanh and Xu, 2020). The corresponding unit cell volume was calculated to be 284.50 Å^3. The electronic band structure of NbFePb, presented in **Fig. 1**, reveals an indirect energy gap of approximately 1.4 eV, located between the valence band maximum at the Γ point and the conduction band minimum at the X point. This small band gap places NbFePb in the semiconductor category, where electron mobility is expected to surpass that of holes. Such a band gap is within the optimal range for photovoltaic applications, which typically spans between 1.0 and 1.6 eV (Bathia, 2014; Fouad *et al*., 2017). Furthermore, the gap aligns with the efficient solar energy harvesting window of 1–2 eV (Dhankhar *et al*., 2014), suggesting NbFePb as a viable material for energy conversion applications.

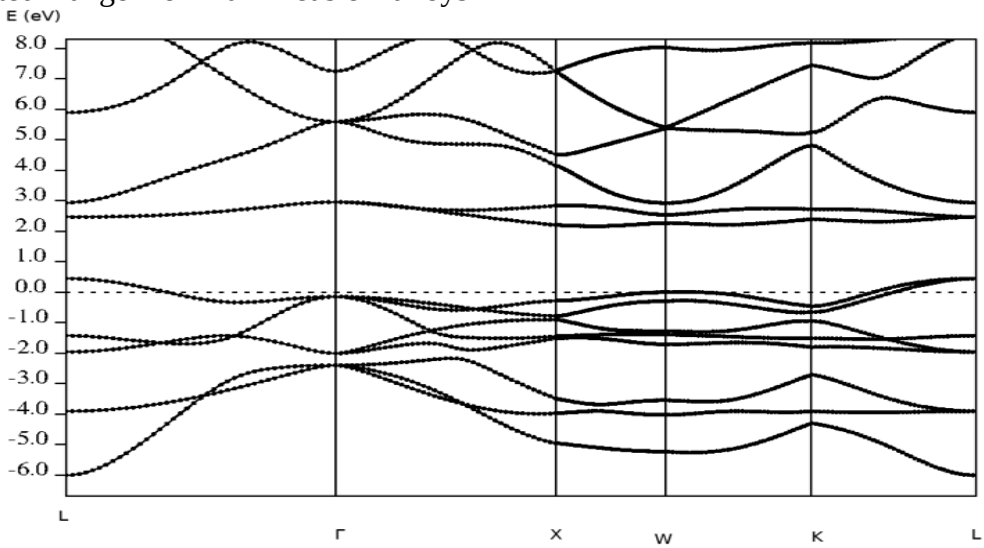

Fig. 1: Band structure diagram of NbFePb compound

The total density of states (TDOS) of NbFePb is shown in **Fig. 2**. A high peak in TDOS is observed around –20 eV, with additional significant states near –30 eV. The strong peak near –20 eV suggests deep bonding states dominated by Pb-related orbitals, while the finite states near the Fermi level confirm semiconducting behavior rather than insulating character. The availability of electronic states close to the Fermi level indicates the potential for moderate electrical conductivity, which is desirable for thermoelectric applications.

The partial density of states (PDOS), illustrated in Fig. 3**,** provides insights into orbital contributions. The Pb-p orbital dominates near –30 eV and close to the Fermi level, playing a crucial role in defining the compound's electronic and transport properties. The

hybridization between Pb-p, Fe-d, and Nb-s orbitals around –18.5 eV indicates strong covalent bonding within the lattice, which enhances structural stability. The coexistence of Nb-d and Fe-d states with Pb-p states near the conduction and valence bands also suggests that electron–phonon interactions may significantly influence the transport behavior. The PDOS further indicates that electron carriers dominate conduction, highlighting the n-type character of the compound.

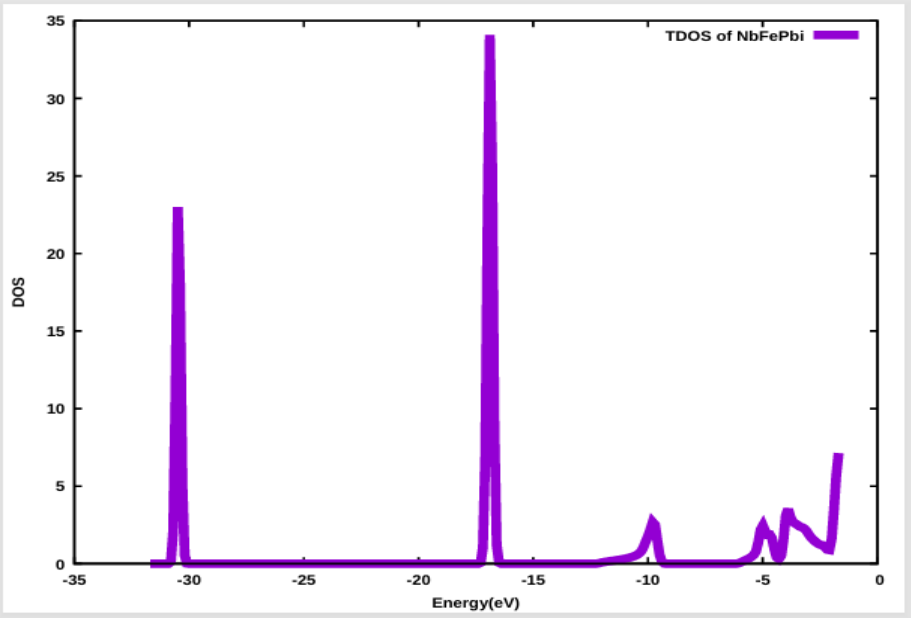

Fig. 2: Total density of states of NbFePb versus Energy

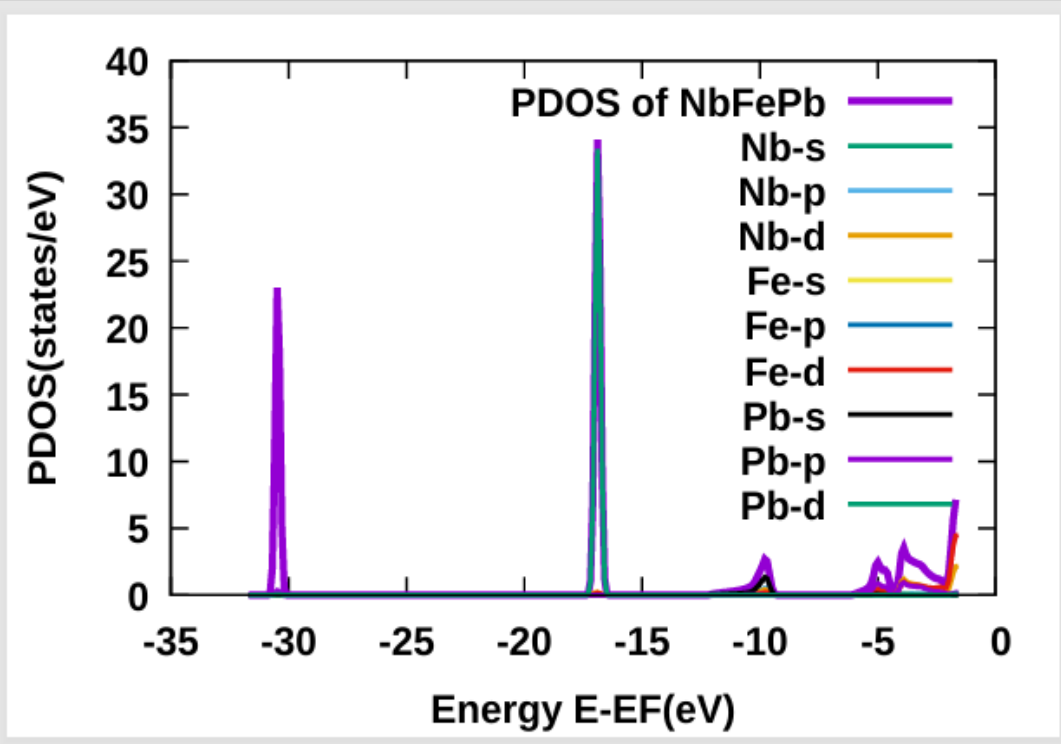

Fig. 3: Partial density of states of NbFePb compound

From these results, the electronic structure demonstrates that NbFePb possesses a favorable band gap, stable orbital hybridizations, and strong density of states contributions that collectively enhance its potential for semiconductor and thermoelectric applications. The hybridization of orbitals further implies improved charge carrier transport, which, when combined with structural durability, can make this material suitable for renewable energy conversion technologies such as waste heat recovery and thermoelectric power generation.

3.2 Thermoelectric Property

The electronic transport properties especially Fig. of merit (zT), Seebeck coefficient(S), electrical conductivity (σ), power factor, electronic fitness function among others which are temperature dependent are examined in this study at temperatures 300K, 500K and 800K. zT quantifies the efficacy of materials to generate thermoelectricity. Thermoelectric materials with high values of zT promotes efficient energy conversion, enhanced solid state cooling and influenced electronic technologies in developing high-impact conductors made with semiconducting materials. zT increased with risen temperature and we recorded very high value of 21, for n-type at 800K as presented in Fig. 4. Variation of Seebeck coefficient as a function of chemical potential was conspicuously disclosed in Fig. 5. For p-type of NbFePb compound, maximum appraisal 2516.96μV/K was observed at temperature of 300K in purple colour follow by 1560.79μV/K at temperature 500K in green colour and 1014.41μV/K in blue colour. All the values of S recorded in this research are far greater than the golden range of 202μV/K to 230μV/K reported by Hong and his co-researchers (Hong *et al*., 2020).

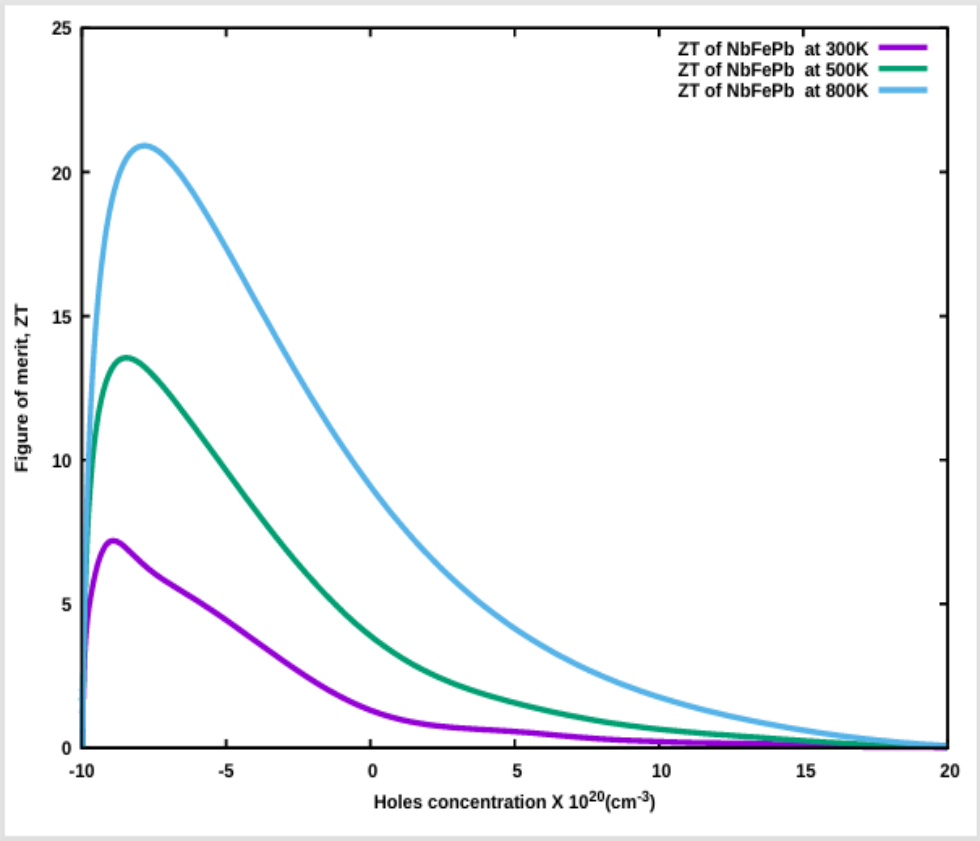

Fig. 4: High-impact Fig. of merit of NbFePb compound versus carrier concentration

Materials with large power factor (PF) connote better thermoelectric performance as it reduces energy wasted in the process of energy conversion. PF controls power inside electronic appliances, enhance efficient operation of components within circuits and improve performance and lifetime of material. High values of PF were calculated at temperatures 800K (21.02W/mK^2), 500K (13.52W/mK^2) and 300K (7.06W/mK^2) and n-type of NbFePb compound is dominant as seen in Fig. 6 which showcase variation of power factor with respect to carrier concentrations (both electrons and holes). Electrical conductivity (σ) differs with material composition, structure, temperature, presence of impurities, carrier concentrations and so on. Measured σ in this work attained its peak value of 4.87S/ms at the minimum temperature of 300K as shown in Fig. 7. Electronic fitness function (EFF) aids in identification and screening of materials with potentials in thermoelectric functionalities. So, materials with improved EFF implies optimum electrical conductivity, Seebeck coefficient and power factor. At electron concentration of -2.4cm^{-3}, EFF rose with varied temperature at 800K and we have estimated value of 0.96. And 0.68 and 0.39 were recorded at temperatures 500K and 300K, both at concentration -23.77cm^{-3} in favour of electron carrier concentration as depicted in Fig. 8.

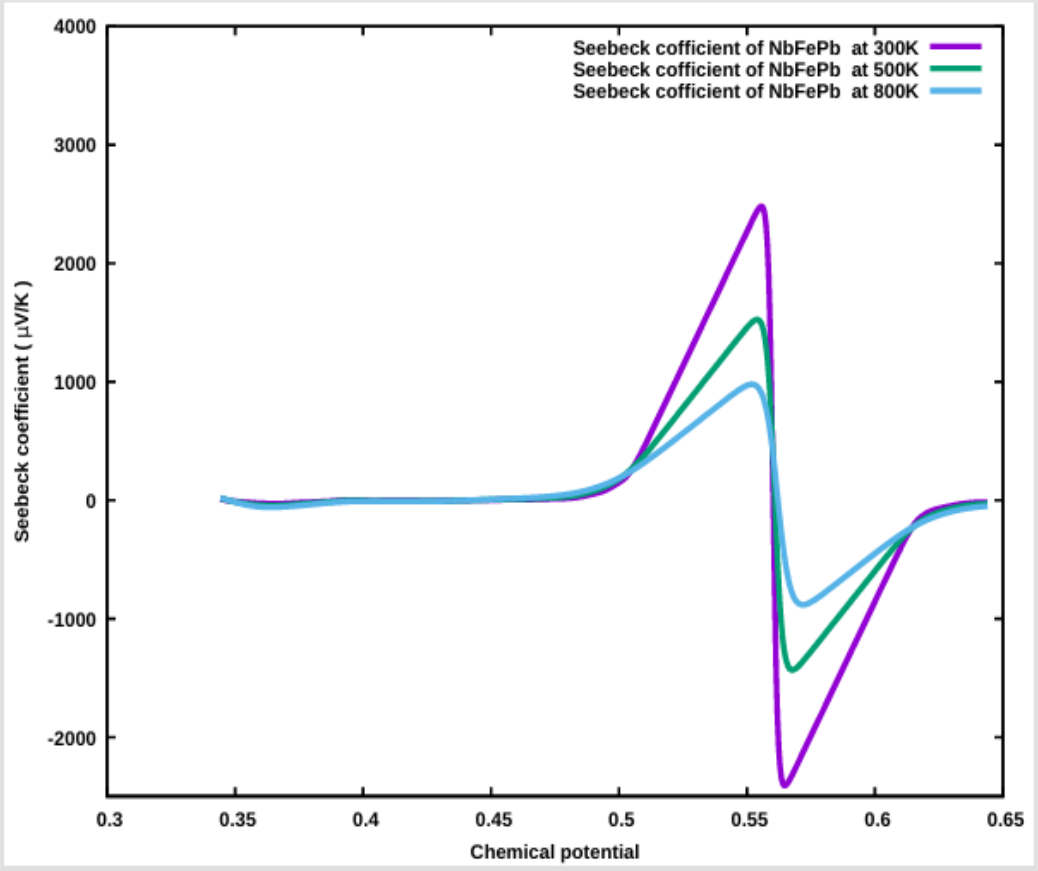

Fig. 5: Variation of Seebeck coefficient with chemical potential of NbFePb compound

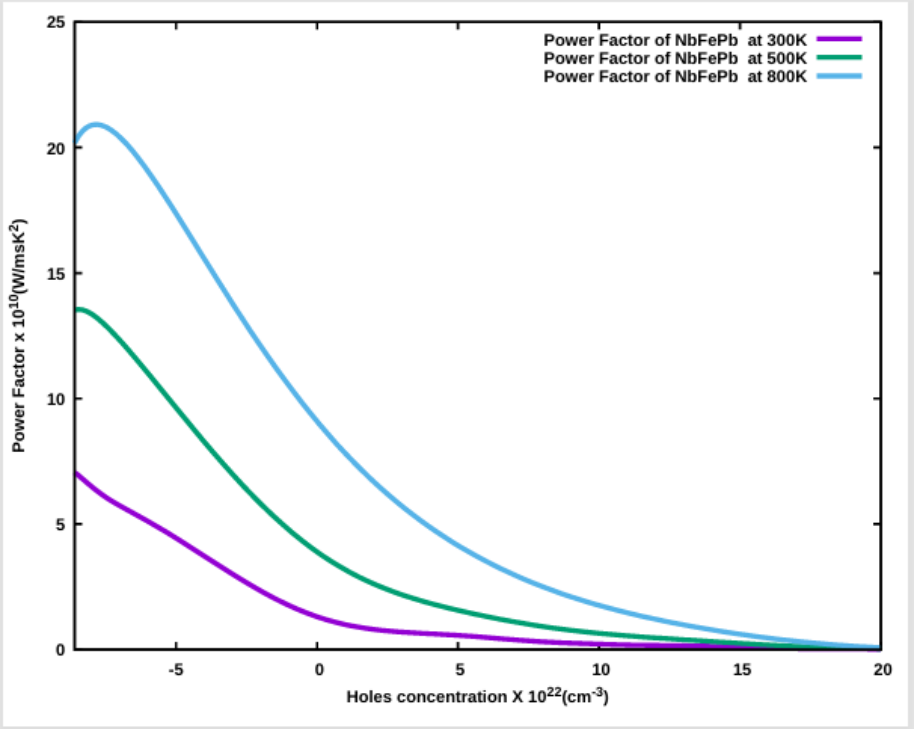

Fig. 6: Power factor of NbFePb compound as a function of carrier concentration

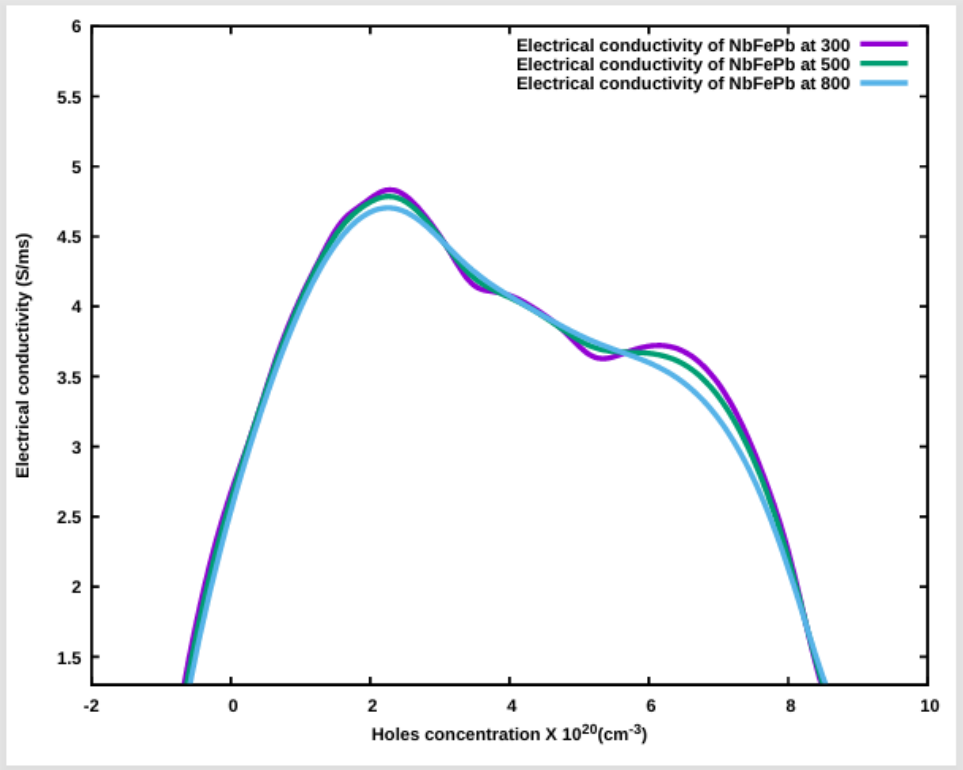

Fig. 7: Diagram of electrical conductivity versus carrier concentration of NbFePb compound

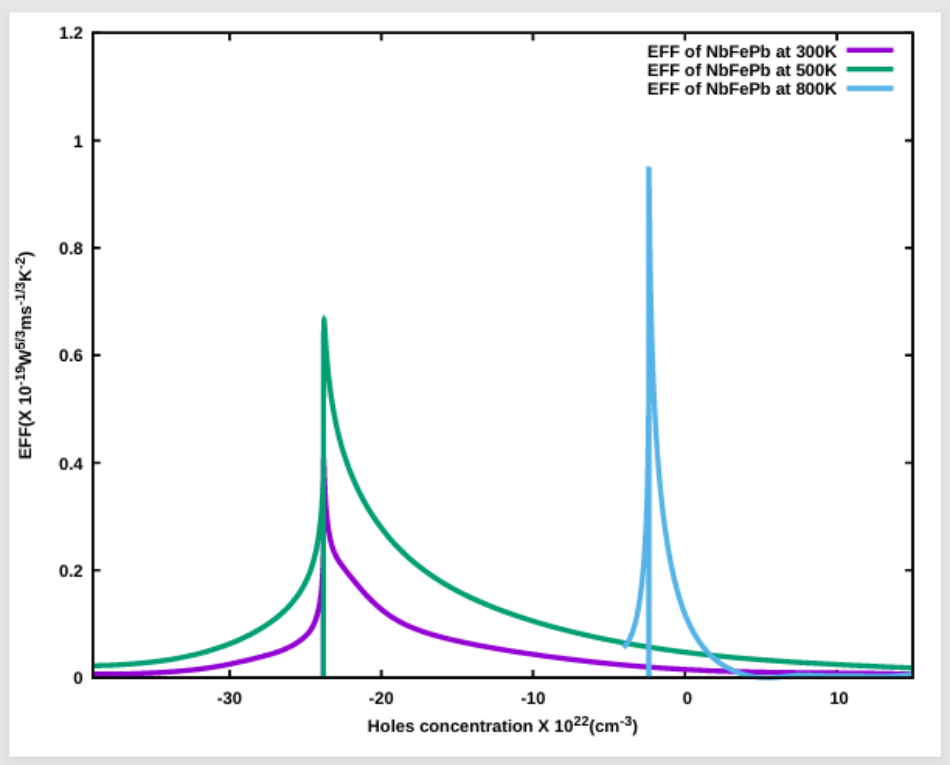

Fig. 8: Variation of electronic fitness functionin connection with carrier concentration of NbFePb compound

3.3 Mechanical and Elastic Properties

Mechanical stability of an unstressed cubic structure is achieved if the material satisfies Born elastic stability criteria (Majumder *et al.*, 2019) expressed as:

$$C_{11} - C_{12} > 0,\ C_{11} + 2C_{12} > 0\ and\ C_{44} > 0 \quad (1)$$

The calculated, positive crystal's elastic energies depicted by stiffness tensor C_{ij} satisfies Born's conditions as evidenced in equation (1) and are enumerated in Table 1. Higher bulk modulus of 325.35GPa and Young's modulus 182.27GPa were documented and this makes this material to be less compressible and resistance to deformation. Dimensionless Poisson ratio 0.44 was computed and this is in harmony with range of material used in Engineering between 0 and 5. Poisson ratio enhances stiffness, strength, stability and vibration of materials.

Table 1: Calculated elastic constants (C_{ij} in GPa), Bulk modulus (B in GPa), Young modulus (E in GPa), Shear modulus (G in GPa) and Poisson ratio (n) of NbFePb

NbFePb	C_{11}	C_{12}	C_{44}	B	E	G	n
This work	497.06	239.49	39.44	325.35	182.27	64.89	0.40

Cauchy pressure (C_p) also known as Cauchy stress tensor portrays the stress state of a material at a point. Estimated C_p is positive (239.49 GPa), this is an indication that NbFePb is ductile. The mathematical expressions for C_p, Anisotropy (A), Universal anisotropy (A^u), Vickers hardness, (V_H) andPugh's (p) ratio are stated in equations (2) to (7)

$$C_p = C_{12} - C_{14} \quad (2)$$

$$\varsigma = \frac{C_{11} + 8C_{12}}{7C_{11} + 2C_{12}} \quad (3)$$

$$A = \frac{2C_{44}}{(C_{11} - C_{12}} \quad (4)$$

$$A^U = \frac{5G_V}{G_R} + \frac{B_V}{B_R} - 6 \quad (5)$$

$$V_H = 2(p^2 G)^{0.585} - 3 \quad (6)$$

and

$$p = \frac{G}{B} \quad (7)$$

Here, B_V, B_R are bulk moduli with regard to Voigt approximation and Reuss approximation, while G_V, G_R are shear moduli with regard to Voigt approximation and Reuss approximation. The ratio of $\frac{B}{G}$ provides insights into a material's behavior under stress. A considerable $\frac{B}{G}$ ratio analyzed in this work which is 5.01 implies high ductility and compressibility of the material, as NbFePb compound is more resistant to volume changes than to shape changes. Kleinman parameter (ς) specifies the relative contribution of bond stretching and bond bending to the overall elastic properties of a material especially its resistance to strain. The evaluated value of ς was 0.25 which implies that bond bending prevails over bond stretching. Anisotropy (A) and Universal anisotropy (A^u), were determined and we noticed NbFePb compound is anisotropy because A is not 1 and $A^U \neq 0$ (Tang *et al*, 2022). Other parameters surveyed are crystal stiffness and Vickers hardness as detailed in Table 2.

Table 2: Computed Cauchy pressure (C_p in GPa), Zener's anisotropy (A), Universal anisotropy (A^u), Kleinman parameter (ζ)Crystal stiffness ($C'' \ in$ GPa) and Vickers hardness (V_H in GPa) of NbFePb

Compound	C_p	A	A^u	ς	C''	V_H
NbFePb	239.49	0.30	1.88	0.24	128.79	0.49

Machinability of NbFePb compound which determines how the material can be cut or shaped for cost effective and innovative designs was also estimated as 8.25.

3.4 Thermodynamics Properties

Thermodynamic property of system defines its thermal behavior and interaction with surroundings. Debye temperature is a functional of covalent bonds in solids; it determines the strength of material and specifies materials with high melting point (Hamidant *et al*., 2009). High melting temperature (T_m) of 3490.67 K was calculated with Θ_D of 296.48K which shows the hardness of this material. The higher the velocity of sound and density of ions, the greater the Debye temperature. The results are presented in Table 3.

Table 3: Calculated density (ρ in g/cm^3), longitudinal velocity, (v_l in m/s), transverse velocity (v_s in m/s), average sound velocity (v_m in m/s), Debye temperature (Θ_D in K) and melting temperature (T_m in K) for NbFePb compound

Material	ρ	v_l	v_s	v_m	Θ_D	T_m
NbFePb	14.12	5.49	0.51	0.58	296.48	3490.67

4.0 Conclusion

This study examined the structural, electronic, thermoelectric, mechanical, elastic, and thermodynamic properties of the NbFePb half-Heusler compound using density functional theory and semi-classical Boltzmann transport approaches. The optimized lattice constant was 5.50 Å with a unit cell volume of 284.50 Å^3. The electronic band structure revealed an indirect band gap of 1.4 eV, within the optimal range for energy harvesting and photovoltaic applications. Density of states analysis showed Pb-p orbitals dominate near the Fermi level, with strong hybridization among Pb, Fe, and Nb states, indicating n-type semiconducting behavior favorable for carrier transport.

Thermoelectric analysis demonstrated exceptional performance. The Fig. of merit (zT) rose with its value, reaching 21 at 800 K, far exceeding conventional thermoelectric materials. The Seebeck coefficient was also remarkable, with values of 2516.96 μV/K at 300 K, 1560.79 μV/K at 500 K, and 1014.41 μV/K at 800 K, greatly surpassing the golden range of 202–230 μV/K from earlier studies. Power factors of 21.02 W/mK^2 at 800 K, 13.52 W/mK^2 at 500 K, and 7.06 W/mK^2 at 300 K were obtained, while peak electrical conductivity reached 4.87 S/ms at 300 K. The electronic fitness function steadily improved with temperature, reinforcing the thermoelectric potential of NbFePb.

Mechanical and elastic properties confirmed NbFePb is durable and ductile. The compound satisfied Born stability criteria, with elastic constants C_{11} = 497.06 GPa, C_{12} = 239.49 GPa, and C_{44} = 39.44 GPa. A bulk modulus of 325.35 GPa and Young's modulus of 182.27 GPa showed strong resistance to compression and deformation, while positive Cauchy pressure (239.49 GPa) and a Pugh ratio of 5.01 indicated ductility. The Poisson ratio of 0.44 aligned with engineering materials, ensuring reliability. The Kleinman parameter (0.25) implied bond bending dominates stretching, while the universal anisotropy factor (A^u = 1.88) reflected anisotropic elastic behavior. Low Vickers hardness (0.49 GPa) suggested good machinability, with a machinability index of 8.25.

Thermodynamic results revealed a Debye temperature of 296.48 K and melting point of 3490.67 K, confirming strong covalent bonding and structural robustness. High sound velocities further supported hardness and thermal stability.

In conclusion, NbFePb combines favorable semiconducting properties, extraordinary thermoelectric efficiency, mechanical durability, ductility, and thermodynamic stability. Its 1.4 eV indirect band gap supports energy harvesting, while the record-high Seebeck coefficient and zT values indicate major potential for waste-heat recovery and solid-state cooling. Mechanical resilience ensures durability in devices, while thermal stability allows operation at high temperatures. These results identify NbFePb as a strong candidate for next-generation thermoelectric and renewable energy applications, warranting experimental validation and device-level integration.

5.0 References

Ayedun, F. (2024). Seebeck coefficient, Fig. of merit, power factor and electronic fitness function as vital tools for assessing thermoelectric behavior of MnNiP compound by first principle approach. *World Journal of Applied Science and Technology, 16*(2), 197-201.

Bathia, S. C. (2014). *Advanced renewable energy systems*. Woodhead Publishing India in Energy.

Casper, F., Graf, T., Chadov, S., Balke, B., & Felser, C. (2012). The band gap can be tuned between 0 and 4eV. *Semiconductor Science and Technology, 27*(6).

Ciftci, Y. O. (2021). Some physical properties of half-Heusler compoundNaYSi: first-principles study. *Journal of Amasya University the Institute of Science and Technology (JAUIST), 2*(2), 32–41.

Dhankhar, M., Singh, O. M., & Singh, V. N. (2014). Physical principles of losses in thin film solar cells and efficiency enhancement methods. *Renewable and Sustainable Energy Reviews*, *40*, 214–223.

Everhart, W., & Newkirk, J. (2019). Mechanical properties of half-Heusler alloys. *Heliyon*, *5*(5), e01578. https://doi.org/10.1016/j.heliyon.2019.e01578

Fouad, M. M., Shihata, L. A., & Morgan, E. I. (2017). An integrated review of factors influencing the performance of photovoltaic panels. *Renewable and Sustainable Energy Reviews*, *80*, 1499–1511.

Giannozzi, P., Baroni, S., Bonini, N., Calandra, M., Car, R., Cavazzoni, C., Ceresoli, D., Chiarotti, G. L., Cococcioni, M., Dabo, I., Corso, A. D., Gironcoli, S., Fabris, S., Fratesi, G., Gebauer, R., Gerstmann, U., Gougoussis, C., Kokalj, A., Lazzeri, M., Martin-Samos, L., Marzari, N., Mauri, F., Mazzarello, R., Paolini, S., Pasquarello, A., Paulatto, L., Sbraccia, C., Scandolo, S., Sclauzero, G., Seitsonen, A. P., Smogunov, A., Umari, P., & Wentzcovitch, R. M. (2009). QUANTUM ESPRESSO: a modular and open-source software project for quantum simulations of materials. *Journal of Physics: Condensed Matter*, *21*(21), 2946590.

Giannozzi, P., Andreussi, O., Brumme, T., Bunau, O., Buongiorno, N. M., Calandra, M., Car, R., Cavazzoni, C., Ceresoli, D., Cococcioni, M., Colonna, N., Carnimeo, A., Dal-Corso, A., de-Gironcoli, S., Delugas, P., Distasio, R. A. Jr., Ferretti, A., Floris, G., Fratesi, G., Fugallo, G., Gebauer, R., Gerstmann, U., Glustino, F., Gorni, T., Jia, J., Kawamura, M., Ko, H. Y., Kokalj, A., Kucukbenli, E., Lazzeri, M., Marsili, M., Marzari, N., Mauri, F., Nguyen, N. L., Nguyen, H. V., Otero-de-la-Roza, A., Paulatto, L., Ponce, S., Rocca, D., Sabatini, R., Santra, B., Schlipf, M., Seitsonen, A. P., Smogunov, A., Timrov, I., Thonhauser, T., Umari, P., Vast, N., Wu, X., & Baroni, S. (2017). Advanced Capabilities for Materials Modelling with Quantum Espresso. *Journal of Physics: Condensed Matter*, *29*(46), 29465901.

Green, M. L. H. (1995). A new approach to the formal classification of covalent compounds of the elements. *Journal of Organometallic Chemistry*, *500*, 127-148.

Hamidani, A., Bennecer, B., & Boutarfa, B. (2009). Structural and elastic properties of the half-Heusler compounds IrMnZ (Z = Al, Sn and Sb). *Materials Chemistry and Physics*, *114*, 732–735.

Hong, M., Lyu, W., Wang, Y., Zou, J., & Chen, Z. (2020). Establishing the golden range of Seebeck coefficient for maximizing thermoelectric performance. *Journal of the American Chemical Society*, *142*(5), 2672–2681.

Khandy, S. A., Kaur, K., Dhman, S., Singh, J., & Kumar, V. (2021). Exploring thermoelectric properties and stability of half-Heusler PtXSn (X = Zr, Hf) Semiconductors: A first principle investigation. *Computational Materials*, *188*, 110232.

Lv, L., Zhao, Y., Ni, J., & Dai, Z. (2024). Comparison of the excellent thermoelectric properties of the half-Heusler compounds RbMgSb with a host-guest structure and LiMgSb. *Results in Physics*, *63*, 107865.

Madsen, G. K., & Singh, D. J. (2006). BoltzTrap. A code for calculating band-structure dependent quantities. *Computer Physics Communications*, *175*(1), 67-71.

Majumder, R., Hossain, M. M., & Shen, D. (2019). First-principles study of structural, electronic, elastic, thermodynamic and optical properties of LuPdBi half-Heusler compound. *Modern Physics Letters B*, *30*(30), 1950378.

Missoum, D. E., Bencherif, K., & Bensaid, D. (2022). First principle investigation of physical properties of MNiBi: (M = Sc, Y)

half-Heusler compounds. *Revista Mexicana de Física, 68*. https://doi.org/10.31349/RevMexFis.68.061601

Mogulkoc, Y., & Ciftci, Y. O. (2017). Investigation on structural, elastic, electronic and vibrational properties of LiTiAl half-Heusler compound using first-principles methods. *Cumhuriyet University Faculty of Science Journal, 38*(2), 312–320.

Mohan, L., Kumar, S. S., Bhardwaj, S. R., & Verma, A. S. (2020). Structural, electronic, mechanical and thermal properties of CoVZ (Z= Si, Ge, Sn, Pb) half-Heusler compounds. *Research in East European Journal of Physics, 4*, 42–50.

Mokhtari, H., Boumia, L., Mokhtari, M., Dahmane, F., Mansour, D., & Khenata, R. (2023). Mechanical stability, electronic and magnetic properties of XzrAs(X = Cr, Mn, V) Half-Heusler compounds. *Journal of Superconductivity and Novel Magnetism*.

Murugan, S. S. (2020). Mechanical properties of materials: definition, testing and application. *International Journal of Modern Studies in Mechanical Engineering, 6*(2), 28–38.

Serrano-Sanchez, F., Luo, T., Yu, J., Xie, W., Le, C., Auffermann, G., Weidenkaff, A., Zhu, T., Zhao, X., Alonso, J. A., Gault, B., Felser, C., & Fu, C. (2020). Exploring Thermoelectric properties and stability of half-Heusler PtXSn (X = Zr, Hf) Semiconductors: A first principle investigation. *Computational Materials Science, 188*, 110232.

Solola, G. T., Bamgbose, M. K., Adebambo, P. O., Ayedun, F., & Adebayo, G. A. (2023). First-principles investigations of structural, electronic, vibrational and thermoelectric properties of half-HeusleeVYGe(Y = Rh, Co, Ir) compounds. *Computational Condensed Matter, 36*, e00827. https://doi.org/10.1016/j.cocom.2023.e00827

Tang, C., Guo, J., Li, B., Kostenevich, A., Wang, L., Rothwell, G., & Ren, J. (2022). In book: Advances in manufacturing processes, intelligent methods and systems in production engineering: 71-85.

Zhang, Y., & Xu, X. (2020). Machine learning modeling of lattice constants for half-Heusler alloys. *AIP Advance, 10*, 045121.

Declaration

Consent for publication

Not applicable

Availability of data

Data shall be made available on demand.

Competing interests

The authors declared no conflict of interest

Ethical Consideration

Not applicale

Funding

There is no source of external funding.

Authors' Contributions

F.A. designed the study, analyzed data, and wrote the initial draft. I.B.A. assisted with analysis and supervised. G.T.S. handled methodology and software validation. M.K.B. performed the investigation and curated data. P.O.A. helped write and edit the manuscript. R.O.A. contributed to visualization and validation. M.S. assisted with analysis and software. I.M.N. handled project administration and resources.